A Proudman-function expansion of the M_2 tide in the Mediterranean Sea from satellite altimetry and coastal gauges

Tides
M_2
Mediterranean Sea
Proudman functions
Geosat

Marée
M_2
Mer Méditerranée
Fonctions Proudman
Geosat

Braulio V. SANCHEZ [a] *, Richard D. RAY [b] and David E. CARTWRIGHT [c]

[a] NASA Goddard Space Flight Center, code 926, Greenbelt, MD 20771, USA.

[b] STX, Goddard Space Flight Center, Greenbelt, MD 20771, USA.

[c] 3, Borough House, Petersfield, Hampshire GU32 3LF, UK.

* *to whom all correspondence should be sent.*

Received 28/02/92, in revised form 4/06/92, accepted 9/06/92.

ABSTRACT

An empirical model has been derived for the semidiurnal principal lunar tide M_2 in the Mediterranean Sea, excluding the Aegean Sea. The work is primarily an exercise in combining satellite altimeter data with tide-gauge data, through the use of specially constructed spatial basis functions. The tide-gauge data consist of M_2 harmonic constants previously derived at 43 chosen coastal locations. The altimeter data consist of approximately two years of Geosat data in the form of collinear differences of sea-surface heights, corrected for orbit error by adjusting long sequences of global data. The tide is expressed as an expansion in Proudman functions - numerically constructed, orthogonal eigenfunctions of the velocity potential. The most important mode is found to be one of period 11.2 hours, presumably owing to its closeness to the tidal excitation frequency.

The resulting M_2 model is shown to be superior to a previous altimeter-based model that had been derived without benefit of spatial basis functions.

Oceanologica Acta, 1992. **15**, 4, 325-337.

RÉSUMÉ

Un développement en fonctions «Proudman» de la marée M_2 en Mer Méditerranée, au moyen de l'altimétrie et des données marégraphiques

Nous avons developpé un modèle empirique de la marée semidiurne principale M_2 dans la Mer Méditerranée, à l'exclusion de la mer Égée. Nous avons réalisé la combinaison des données altimétriques et marégraphiques à l'aide d'une représentation spatiale sur une base de fonctions. Les données marégraphiques sont des constantes harmoniques de 43 sites côtiers sélectionnés. L'altimétrie provient de presque deux ans de la mission Geosat, analysée sous la forme de différences colinéaires, dont les erreurs d'orbite sont réduites par ajustement de longues séries globales de données. On exprime la marée sous la forme d'un développement en fonctions de Proudman - fonctions propres orthogonales du potentiel de flux. Le mode principal se trouve à la période de 11,2 heures, probablement à cause de sa proximité à la fréquence de l'excitation.

On montre que le modèle pour M_2 est de qualité supérieure à un modèle précédent basé sur l'altimétrie, mais n'utilisant pas le procédé de synthèse spatiale.

Oceanologica Acta, 1992. **15**, 4, 325-337.

INTRODUCTION

Being relatively weak, there have been few attempts to model the tides of the Mediterranean as a whole. Early twentieth century studies by Sterneck and Defant (summarized by Defant, 1961) established the broad outlines: the tide is mainly semidiurnal with standing-wave regimes in four large basins separated by narrow nodal zones near Alicante, Tunis, and Crete, together with shallow-sea resonances at the head of the Adriatic and in the Gulf of Gabes. The Adriatic also resonates to the otherwise weak K_1 tide. It was clear to Defant (1961) that, contrary to earlier belief, the Mediterranean tide is mainly generated by the action of the tidal forces on the Sea itself, although he considered that the Atlantic tide feeds a significant amount of energy through the Strait of Gibraltar.

Maloney and Burns (1958), on the other hand, examined the progression of the tide near Gibraltar Strait and concluded that the Atlantic tide is entirely reflected back into the ocean and, in their view, plays no part in the Mediterranean system. In terms of energy transmission, this view has been partly vindicated by Candela (1989, Ch. 1, § 6) through extensive measurements of tidal currents in the Gibraltar experiment, which demonstrated zero net flux of M_2 energy through the strait; the barotropic tidal flow is in quadrature with the elevation. This important result is of course not the same as the effect of a rigid barrier. The western Mediterranean does co-oscillate with the Atlantic tide, but all dissipated energy must be provided by the action of the tidal forces on the whole Sea.

The only numerical model of the M_2 tide in the Mediterranean Sea, to our knowledge, is that of Dressler (1980). Dressler applied the HN formulation of the Hamburg school (Hansen, 1962; Zahel, 1970) to a 1/3° grid in latitude and longitude, with forcing only from the tilt of the tidal potential surface. In one experiment, the model was run with the Gibraltar Strait "closed"; in another it was "open", but with specified elevation. Dressler's tidal map for the open case agrees better than that for the closed case with coastal data from the basins west of Sicily, but east of Sicily the tide is practically unaffected. However, the coastal data then available was unevenly distributed and variable in quality. The model gave poor results for the head of the Adriatic, but these were improved by a separate, finer scale model of the Adriatic Sea alone with forcing at Otranto Strait.

Since Dressler's work, more coastal tidal data have been published and the harmonic constants for some ports have been improved by analysis of longer records (*e.g.*, Purga *et al.*, 1979). New data for the open Mediterranean Sea have also become available through the analysis of satellite altimetry (Cartwright *et al.*, 1991), as part of a global program. However, the altimetric data are close to the noise threshold, and are absent from some of the narrower regions, and so require a model for optimum representation. In the present paper, we seek to incorporate both satellite and tide gauge data in a numerical model of the Mediterranean, using an objective method which has proved effective in oceans and seas of greatly different sizes, from Lake Superior (Sanchez *et al.*, 1985) to the Pacific Ocean (Sanchez and Cartwright, 1988). Indeed, the Mediterranean Sea provides an interesting contrast to both these extremes in size and complexity.

Essentially, our method is to fit the data optimally to a set of spatial eigenvectors of the barotropic velocity potential, known as Proudman functions. The Proudman functions are mutually orthogonal and they individually satisfy mass conservation over the computed basin area. They provide in principle a complete description of the elevation field of any harmonic tide component. The associated vorticity modes, which arise from the same formalism as the Proudman functions but with strictly zero horizontal divergence, are irrelevant to the problem in hand, although they may be necessary to define the field of horizontal transport.

In the following section, we first describe the computation of Proudman functions for the Mediterranean, and then compare their spatial structures and natural periods with known related features of the sea. Comparison is also made with equivalent functions computed by Schwab and Rao (1983) over a somewhat coarser grid. In succeeding sections we describe the available tidal data in more detail and discuss how they are used to constrain the model and the resulting tidal maps.

PROUDMAN FUNCTIONS

Proudman functions, which will be used here as basis functions in the tidal estimation, have been described in several papers (*e.g.*, Rao and Schwab, 1976). The formalism for these functions needs to be reviewed here only briefly. Essentially, the Proudman functions are velocity potential functions that are solutions to the following eigenvalue problem:

$$\nabla . h \nabla \phi_i = - \lambda_i \phi_i \qquad (1)$$

with boundary conditions

$$h \frac{\partial \phi_i}{\partial n} = 0 \qquad (2)$$

where h is the (variable) basin depth, $\partial/\partial n$ is the gradient normal to the basin boundary, and ϕ_i is an eigenvector with corresponding eigenvalue λ_i. The left-hand-side of equation (1) is the divergence of the transport vector; the operator is self-adjoint and hence has real eigenvalues and orthogonal eigenvectors. Given the equation of continuity, it can be shown that these eigenvectors provide a sufficient basis for the tidal heights.

The ϕ_i functions are in fact the gravitational normal modes for a fluid in a non-rotating basin (Rao and Schwab, 1976). They have the character of standing waves with periods obtainable from the eigenvalues λ_i.

The solution of equation (1) for basin models with realistic boundaries and bottom topography must be obtained by numerical techniques. In the present investigation the solution was computed using finite differences on a 0.5° grid, the latter comprising 956 velocity-potential points. The bathymetry data were obtained from the 5' database of the World Data Center, Boulder; after averaging, these depths ranged from a maximum 4 238 m to a (preset) minimum 100 m. We have excluded the Aegean Sea from the analysis, primarily because we know of no available harmonic constants from tide gauges there; exclusion of the Aegean also facilitates direct comparisons to the normal mode calculations of Schwab and Rao (1983), who had excluded the Aegean in their study, Dressler's (1980) calculations suggest that the Aegean is a distinct tidal regime with an abrupt border at Crete). Although the Adriatic Sea is included, we find, as did Schwab and Rao (1983) and Dressler, that our 0.5° resolution is insufficient to represent properly the amphidromic tidal structures there. Our grid also represents the Strait of Gibraltar as closed. Such unrealistic boundary conditions may be expected to degrade the solution somewhat in the western Alboran Sea. Closure of the Strait also eliminates the possibility of a Helmholtz-type mode with the entire Mediterranean co-oscillating with the Atlantic.

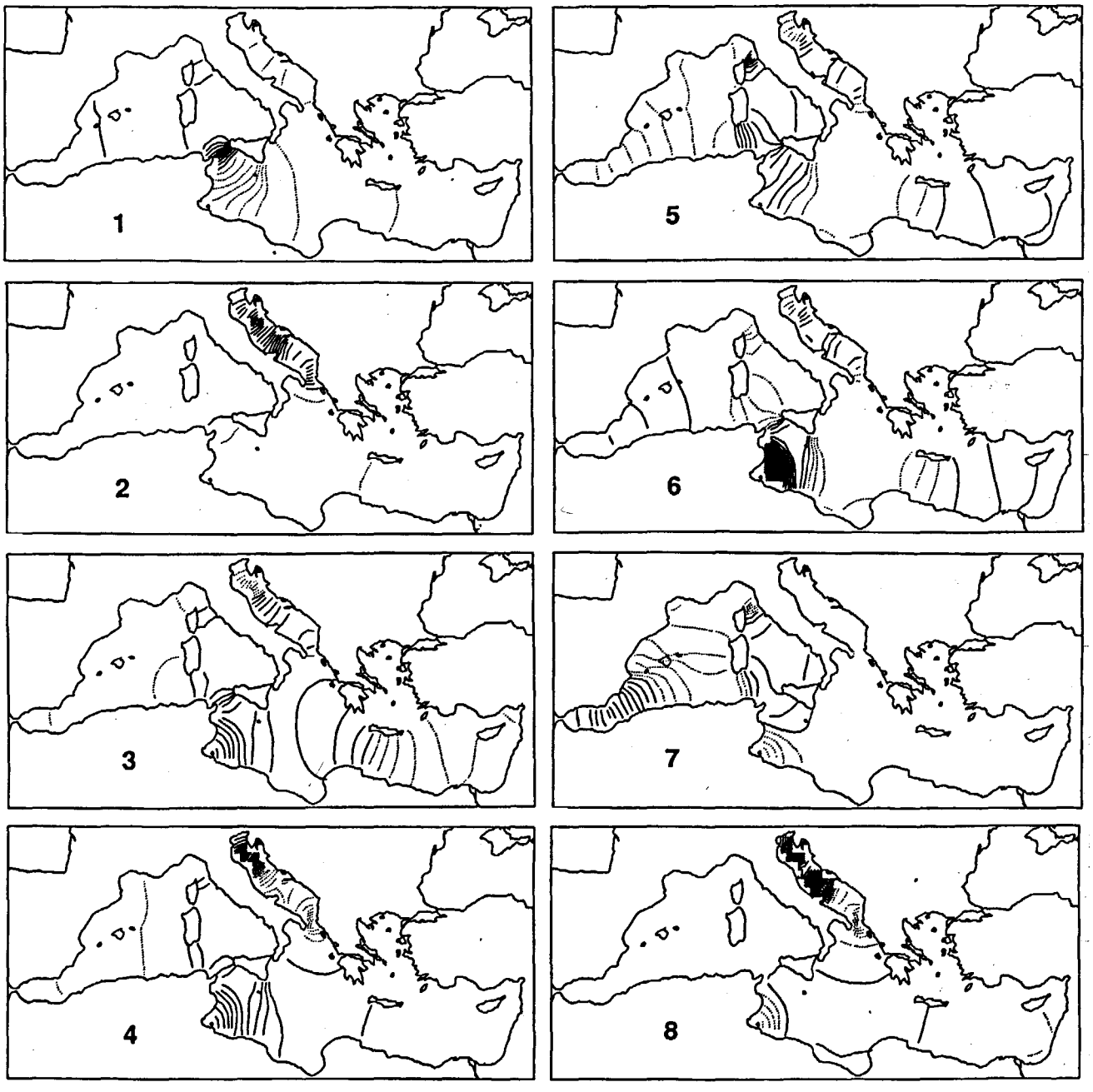

Figure 1

Mediterranean Proudman functions 1-8. The solid and dotted lines denote contours of opposite sign. The contour interval is arbitrary, since for display purposes, only the shapes of these functions are of concern. The functions are ordered according to their period. Function 1 is a half-wave with a nodal line across the Sicily Strait, and each function thereafter shows increasingly complex structure.

Table 1

Zero-rotation gravitational modes (Proudman functions) of the Mediterranean.

			Relative mean potential energy in basin					
Proudman function	**Period (hr)**	**Period * (hr)**	**Balearic Basin**	**Tyrrhenian Sea**	**Adriatic Sea**	**Gulf of Gabes**	**Ionian Basin**	**East of Crete**
1	38.61	42.5	1.9	1.3	1.0	0.1	0.5	0.7
2	21.07	20.0	0.0	0.0	15.8	0.1	0.1	0.3
3	11.17	11.3	0.1	0.1	2.3	5.0	0.8	1.7
4	9.87	9.3	0.1	0.2	13.7	3.3	0.2	0.0
5	8.50	8.4	1.0	4.7	0.9	0.6	0.4	0.2
6	7.78	7.3	0.2	1.0	0.8	13.1	0.8	0.3
7	6.09	6.8	3.5	0.9	0.0	0.4	0.0	0.0
8	5.77		0.0	0.0	16.9	0.3	0.1	0.0
9	5.20		0.0	0.6	0.1	16.1	1.1	0.0
10	4.35		0.0	0.0	0.2	9.1	1.4	1.0
11	4.13		0.0	0.0	10.5	0.9	0.2	1.2
12	4.08		0.0	0.0	6.5	3.2	0.6	1.4
13	3.78		3.5	0.9	0.0	0.2	0.0	0.0
14	3.69		0.0	0.0	0.7	3.0	2.7	0.1
15	3.56		0.0	0.3	0.1	18.2	0.9	0.0
16	3.44		3.7	0.5	0.0	0.1	0.0	0.0
17	3.18		3.2	1.3	0.0	0.4	0.1	0.0
18	3.17		0.0	0.0	11.0	0.0	0.1	1.4
19	3.15		0.1	0.0	6.0	0.1	0.1	2.5
20	3.04		0.8	2.0	0.2	5.4	1.1	0.1

** from Schwab and Rao (1983).*

Figure 2

Locations of tide gauges from which M_2 harmonic constants have been utilized in this study. Dashed lines delineate the six regions used in Table 1.

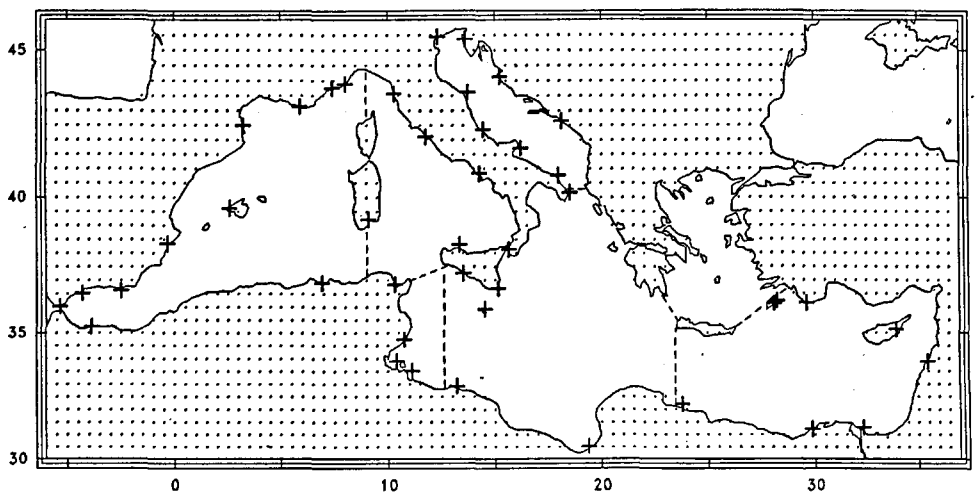

The solution of equation (1) for the Mediterranean yields a wide spectrum of Proudman functions, ranging from a zeroth mode - a constant function with very long numerical period (infinity in the continuous theoretical limit) - to the 955th mode with period 9.9 minutes (the constant mode was not used in the tidal estimation below.) Figure 1 displays the first 8 Proudman functions (excluding the zeroth mode), each function showing progressively more complicated spatial structure with decreasing period. Table 1 lists the periods of the first twenty functions. Column 3 of Table 1 shows the corresponding periods obtained by Schwab and Rao (1983).

The remaining columns of Table 1 list the relative mean potential energies of the waves in several regions of the Mediterranean, the domain of these regions being shown in Figure 2. These means were computed as

$$\frac{\int_{Ai} \phi^2 \, dA/A_i}{\int_A \phi^2 \, dA/A}$$

where A denotes the total area of the Mediterranean and Ai is the area of a particular region. A wave of constant amplitude would have an entry of 1 for each of the six regions, while greater than 1 denotes greater relative potential energy for that region and vice versa. An inspection of Table 1 indicates that Proudman functions number 2, 4, 8, 11, and 18 are essentially Adriatic waves while functions number 6, 9, and 15 are mostly energetic in the shallow Gulf of Gabes and adjoining areas east of Tunisia. Functions number 7, 13, 16, and 17 are more pronounced in the Balearic Basin. Function number 5 is localized in the Tyrrhenian Sea.

Schwab and Rao (1983) do not give diagrams showing their computed Proudman functions, but they do show their three gravest normal modes (*i. e.*, with earth rotation). These correspond in period to our modes 1, 3, and 5 - modes 2 and 4 being essentially Adriatic modes. Schwab and Rao emphasize the small role rotation plays in the per-

Figure 3

M_2 amplitudes (top) and Greenwich phase lags (bottom) derived by interpolation of coastal tide gauges with an expansion in 10 Proudman functions. Amplitudes in cm, phases in degrees.

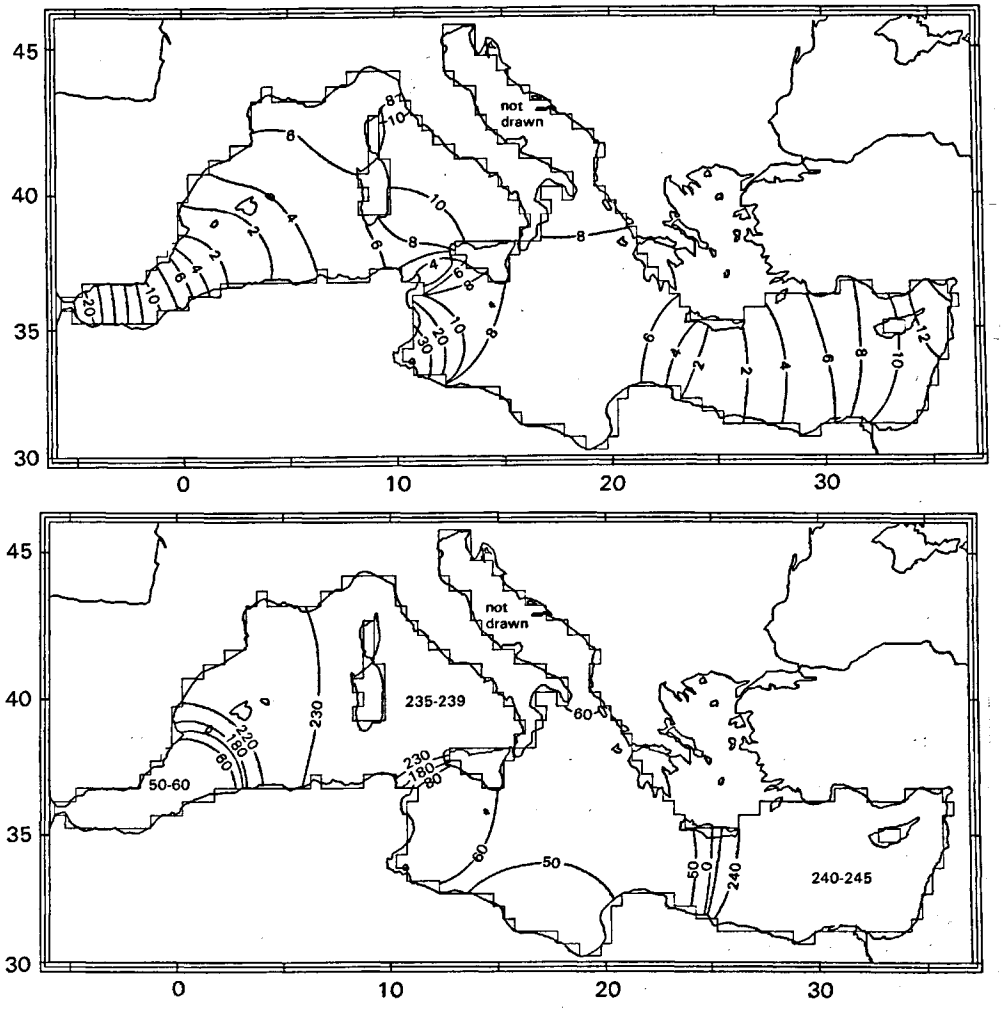

iods of their normal modes: 38.5, 11.4, 8.4 hours compared to 42.5, 11.3, and 8.4 hours for the non-rotating case (Tab. 1, column 3). Similarly, rotation only weakly affects the geometrical structure of the modes. This is confirmed by direct comparison of Schwab-Rao Figures 3, 4, and 5 to our Figure 1 wherein each of our nodal lines in modes 1, 3, and 5 is found transformed into an amphidrome, but often with such rapid phase progression as to be essentially a standing-wave system. The locations of these nodal positions are in all cases in good agreement, and amplitude gradients are found to be in the same sense.

INTERPOLATION OF COASTAL HARMONIC CONSTANTS

As an inital application of the Mediterranean Proudman functions, we have used them to provide spatial basis functions for interpolating the M_2 tide throughout the Mediterranean Sea from the harmonic constants of selected tide gauges. This is an elementary least-squares exercise, but the resulting maps will provide a useful background from which to evaluate the altimeter-derived tide.

Harmonic constants from 43 coastal tide gauges were selected for this purpose, the majority taken from the databank of the International Hydrographic Organization (IHO), Monaco. The stations were selected according to the date of the original measurements, the timespan of the measurements, and the uniformity of coverage across the Mediterranean. No accepted measurements predate 1920, although for three stations in the Alboran Sea no times were listed. Most stations were of at least one year duration, although six were of only one month. The IHO lists were also supplemented by constants taken from the publications by Purga *et al.* (1979) and Mosetti and Purga (1989; 1990) and Rickards (1985). The constants for Beirut were taken from Defant (1961); they provide the only measurements along the eastern boundary of the sea, but the original source for these measurements and their quality is unknown. Harmonic constants for Banyuls were chosen in

Table 2

Fit statistics for tide gauges only.

N	ν	rms (cm)	χ^2/ν (cm^2)
6	74	4.32	5.42
7	72	3.51	3.68
8	70	3.51	3.78
9	68	3.43	3.72
10	66	3.01	2.95
11	64	2.98	2.98
12	62	2.94	3.00
14	58	2.88	3.08
16	54	2.70	2.90
18	50	2.65	3.02

preference to nearby Port-Vendres (Rickards, 1985) because Banyuls data covered two full years (1968-1969), whereas Port-Vendres had only nine months, and we suspect a time-zone error in its phase lags. Finally, one station - Islas Chafarinas, off the coast of northeast Morocco - was originally selected from the IHO lists but was discarded after it produced consistently high residuals in our fits and seemed discordant with neighboring measurements. The 43 selected stations are shown in Figure 2.

Let H and G be the amplitude and Greenwich phase at any station (most data sources used local phases κ or g, requiring conversion to G). Let $H_1 = H \cos G$ and $H_2 = H \sin G$ be the tidal components inphase and in quadrature, respectively, with the tide generating potential at Greenwich. These quantities are then expanded in Proudman functions as

$$H_1(\varphi, \lambda) = \sum_{i=1}^{N} a_i \phi_i(\varphi, \lambda)$$

$$H_2(\varphi, \lambda) = \sum_{i=1}^{N} b_i \phi_i(\varphi, \lambda) \qquad (3)$$

where a_i and b_i are determined by least squares. All stations were equally weighted, there being no error estimates assigned in most sources. Essentially the only adjustable parameter is N, the degree of fit. Statistics for a number of different N are summarized in Table 2. The χ^2 statistic is computed in the usual manner as

$$\chi^2 = \sum_j [\text{observed } (j) - \text{computed } (j)]^2/\sigma^2,$$

summing over all stations, where we have set the noise variance σ^2 somewhat arbitrarily to (2 cm)^2. The so-called "reduced χ^2 statistic", χ^2/ν with ν the number of degrees of freedom in the fit, levels off near a natural choice of N = 10. Its magnitude, however, is rather large (*cf.* tables of the χ^2-distribution in standard handbooks, *e. g.*, Snedecor and Cochran, 1989), and indicates that either σ is too small or our model is incorrect. In fact, the latter must be partially true, since most of the larger residuals occur in the Adriatic and the approaches to Gibraltar where, as noted above, the present Proudman functions are expected to be either inadequate in resolution or inaccurate in assumed boundary conditions. Eliminating from the statistics (but not from the fit) Gibraltar and the three stations in the Alboran Sea and the four stations in the northernmost Adriatic gives an rms residual of 2.5 cm. Additionally eliminating the three stations from the resonant, high-tide Gulf of Gabes from the statistics gives an rms residual of 1.5 cm, which is a satisfactory fit to the majority of stations.

The interpolated M_2 tide, in amplitude and Greenwich phase lag, is shown in Figure 3. The phase map (bottom figure) in particular clearly delineates the basin into a series of standing waves, with remarkably constant phase lags over large regions separated by narrowly defined nodal regions. The exact behavior in some of the nodal regions, *e. g.* whether the phases progress eastward or westward south of Crete, would require more detailed local observations, and, in any event, is physically insignificant owing to the corresponding small amplitudes. As noted above, the 1/2° resolution of the Proudman functions is inadequate to capture the complex tidal structure in the Adriatic. Thus, we leave this region blank to prevent casual readers being misled by overly smoothed results.

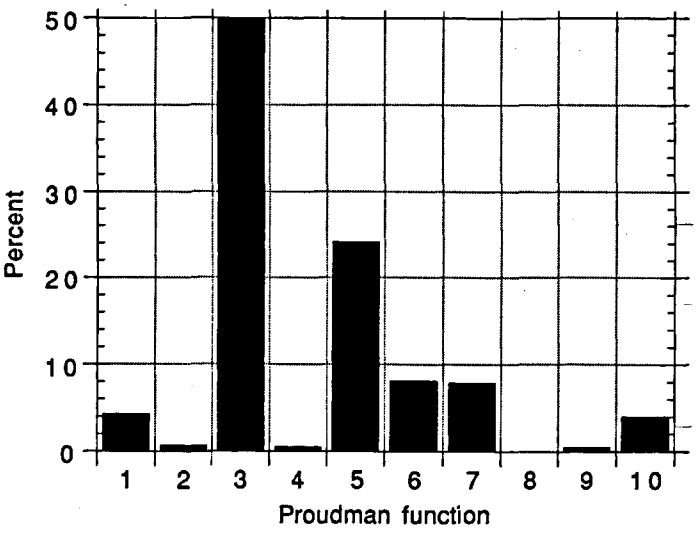

Figure 4

Percentage of potential energy contributed by each Proudman function in the fit to tide-gauge data only.

Each of the Proudman functions included in the summations of equations (3) contributes a certain percentage to the overall potential energy of the tide, according to

$$(\text{P.E.})_i = 100 \times \frac{a_i^2 + b_i^2}{\sum_{j=1}^{N} a_j^2 + b_j^2}$$

These contributions have been evaluated and are shown in the histogram of Figure 4. Two modes clearly predominate: modes 3 and 5, both of which were depicted in Figure1. We defer further discussion of Figures 3 and 4 to the final section.

At this point it may be of interest to describe a separate exercise in which the present tide-gauge data were fit to a second set of Proudman functions that had been computed with constant depths (taken as 1 442 m, as in the "constant depth" calculations of Schwab and Rao, 1983). Such functions are still orthogonal and still conserve mass, but they do not properly incorporate kinematic constraints as realistically as do the functions in Figure 1. Fitting the tide-gauge data to N = 16 of these functions resulted in an rms residual of 4.4 cm, to be compared to 2.7 cm from Table 2 and 4.3 cm for N = 6. The obvious conclusion is that realistic modes offer superior efficiency in data fitting. Their use may be preferable to purely statistical interpolation methods, particularly those that assume stationary and isotropic covariances.

TIDAL DETERMINATION FROM ALTIMETRY

Satellite altimeter data from the Geosat Exact Repeat Mission (ERM) have previously been used to study the ocean tides, on both global scales (*e. g.*, Cartwright and Ray, 1990) and regional scales (*e. g.*, Woodworth and

Thomas, 1990). In its use of Proudman basis functions, the present study follows Sanchez and Cartwright (1988), whose analysis of the M_2 and O_1 tides in a wide expanse of the Pacific was encouraging, but limited by the need for artificial southern boundaries and by the short duration of the Seasat mission. We have here used approximately two years of ERM data, from 8 November 1986 to 8 October 1988 (although with about twenty days of omissions or deletions).

The ERM groundtracks for the Mediterranean area are shown in Figure 5. This track pattern was repeated every 17.05 days, commencing 8 November 1986 and continuing until the end of the Geosat mission in late 1989. Unfortunately, owing to hardware difficulties described by Cheney *et al.* (1988), data are not always available from each satellite pass. Figure 6 shows a "density plot" that displays the relative amounts of usable Geosat passes in each 1° x 1° square throughout the area, with darker squares denoting greater numbers of usable data. The western basin, and particularly the Alboran Sea, is seen to be sparsely covered; implications of this will be commented on below.

For the basic processing of the Geosat altimeter data - in fact, up to the point at which the tidal analysis is performed - we have followed closely the methods described in Cartwright and Ray (1990). The basic variable for analysis is $\Delta\xi$, formed from two measured sea surface heights at the same position but with constant time offset:

$$\Delta\xi(\varphi, \lambda, t) = \xi(\varphi, \lambda, t) - \xi(\varphi, \lambda, t + n\tau) \qquad (4)$$

where φ and λ are latitude and longitude, τ is the ERM repeat period (17.0505 days) and n is a small integer (taken as 2 in the present study). Owing to the exact (within 1 km) repeat of the groundtrack, equation (4) removes from the analysis the dominating geoid signal (plus otherstatic terms) at the trivial expense of transforming - in an exactly known manner - the amplitude and phase of the tidal signal in ξ to a modified signal in $\Delta\xi$. The integer n can be chosen to optimize this transformation to enhance the signal of interest (Cartwright and Ray, 1990).

Altimeter corrections

A multitude of corrections must be applied to the altimeter measurements in order to yield accurate estimates of ξ (Cheney *et al.*, 1987). Many of these corrections are routine, and only a few require comment here.

The Automatic Gain Control (AGC) (not itself a correction term) is often used to avoid the presence of sea ice within the altimeter footprint, data being rejected when AGC > 36 db (Marsh and Martin, 1982). In the Mediterranean, however, where there is no danger of ice, AGC can often exceed 36 db. At such times, the surface of the Mediterranean is apparently so calm that the returned radar waveform is unusually strong (and its leading edge unusually sharp), but the height measurements are nonetheless reliable. Because of this, AGC editing was removed to avoid unwarranted data loss in this area.

A somewhat controversial correction is for atmospheric loading. In general, as a global average, it is known that a

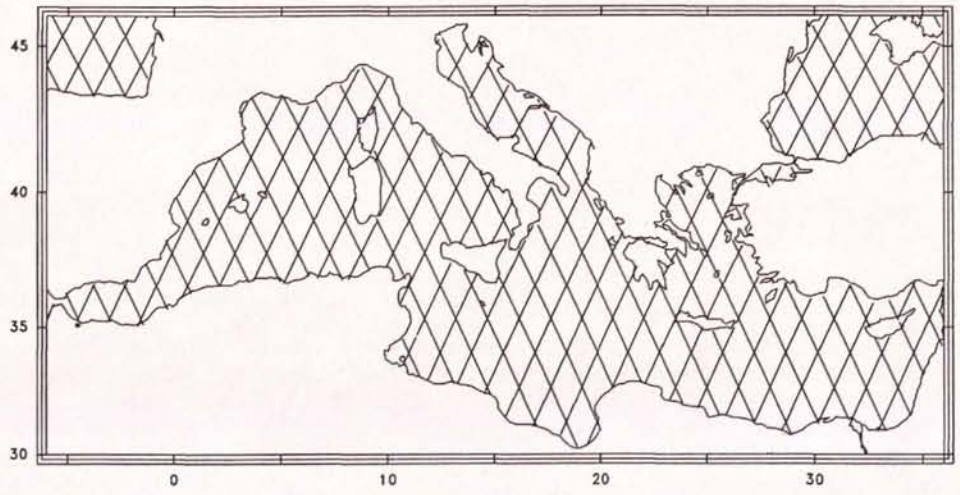

Figure 5

Satellite groundtrack during the Geosat Exact Repeat Mission. Ascending (or descending) tracks are 360/244 = 1.4754° apart in longitude. This track pattern was repeated every 17.05 days.

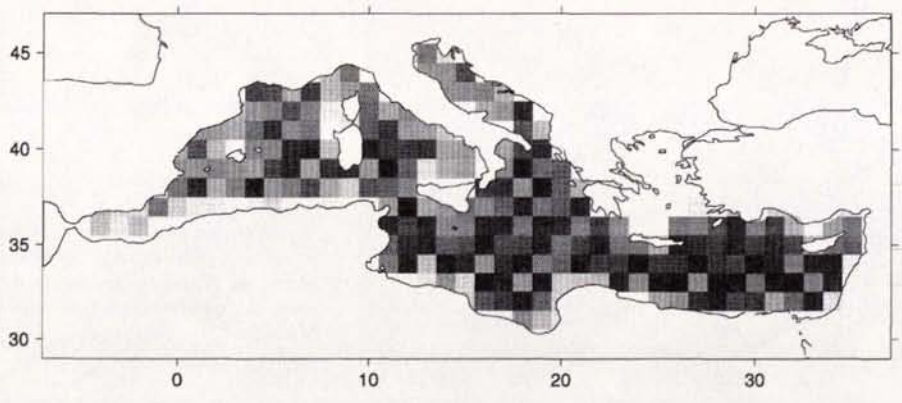

Figure 6

Density plot showing relative coverage of usable Geosat passes in each 1° x 1° area of the Mediterranean. Darker squares indicate higher numbers of observations; white squares denote no observations.

static inverted barometer correction (*e. g.*, Cheney *et al.*, 1987) produces large (~ 50 cm^2 or more) reductions in variance for $\Delta\xi$ (Ray *et al.*, 1991). This represents a considerable noise reduction. Within the confines of the Mediterranean Sea, however, an inverted barometer response is more questionable, because the constriction at the Strait of Gibraltar limits the amount of flow necessary to attain adjustment with atmospheric pressure. The problem has been studied by Garrett and Majaess (1984), who found that sea level response in the Mediterranean is isostatic at very low frequencies when there is sufficient time for the necessary flow through the Strait and at high frequencies where smaller atmospheric spatial scales allow internal adjustment within the sea. Near periods of 100 hours, however, they found definite nonisostatic response. This is unfortunately a period typical of many meteorological systems. Applying and not applying the inverted barometer correction are therefore both something of a compromise, and, in the end, we did apply the correction.

Another correction that requires consideration, particularly in a discussion of tides, is the load tide. A satellite altimeter is sensitive only to the geocentric tide, that being the sum of the body, ocean, and load tides. Although a geocentric tide is useful in certain applications, especially for removing tidal signals from altimeter data in preparation for other oceanographic studies, it is usually the "ocean tide" - the tide relative to the sea bottom - that is desired. This is certainly so when tide-gauge data are to be combined with altimetric data, as below. To obtain the ocean tide from the geocentric tide, both body tides and load tides must be computed and subtracted. The body tide is computed directly from the tide-generating potential and is straightforward, but the load tide is more problematic. The load tide at any point depends not only on the immediately adjacent ocean tide, but on the complete global tide; in fact, the loading Green's function at a spherical distance of 180° has a magnitude half that at 1° (Farrell, 1972). In Cartwright and Ray (1991), the load-tide correction was applied after the combined (ocean + load) tide had first been determined, an acceptable procedure given the near-global expanse of those models. In the present application, one could use a load-tide based on the Schwiderski (1983) model (Ray and Sanchez, 1989), but the Schwiderski model is undefined in the Mediterranean Sea. Instead, we have applied a load-tide correction given by Cartwright *et al.* (1991, Fig. 3.4), which is based on both global and local Mediterranean data. This load tide has an amplitude of approximately 5 mm in the eastern Mediterranean, increasing to 10 mm in the Alboran Sea, then rapidly to approximately 25 mm at Gibraltar.

The final correction concerns radial orbit error. The satellite orbital positions necessary to obtain ξ were based, as in

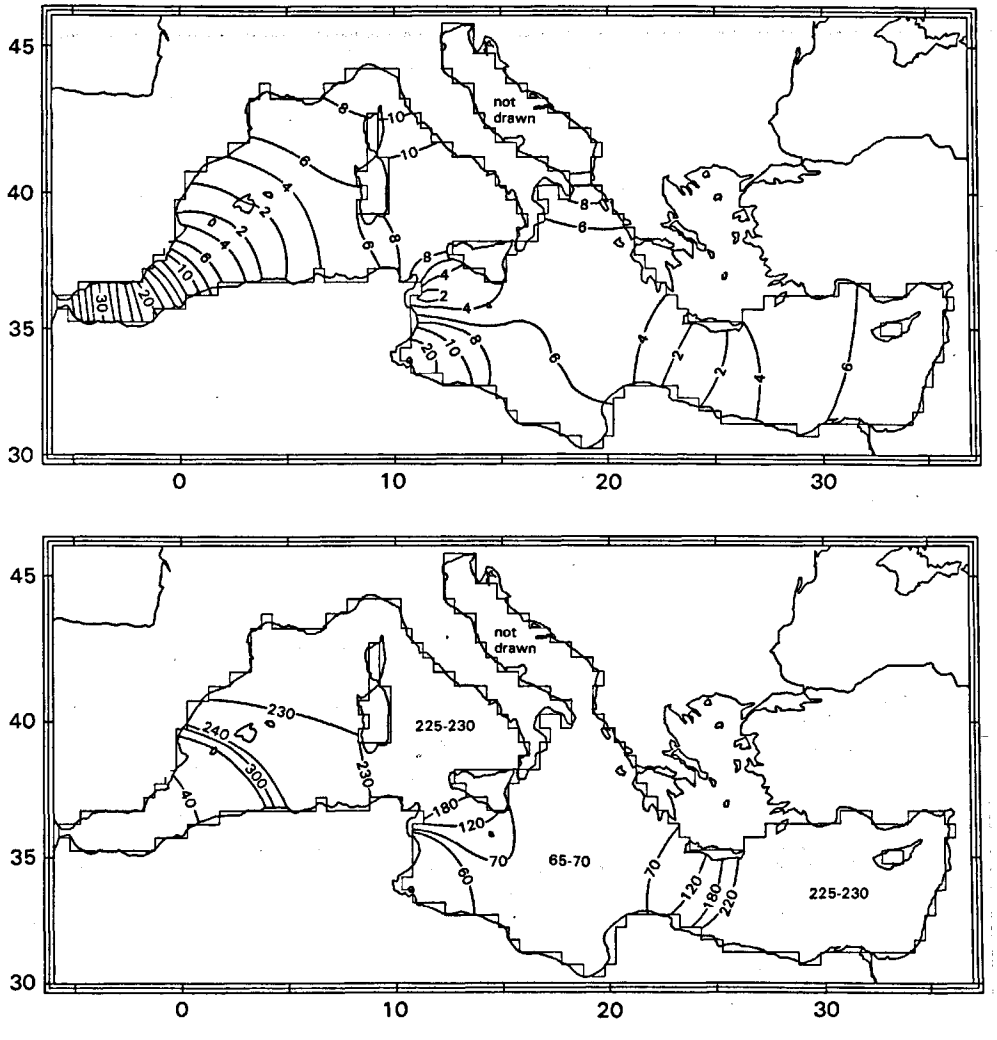

Figure 7

M_2 amplitudes (top) and Greenwich phase lags (bottom) derived from (only) the Geosat altimeter data, using an expansion in 10 Proudman functions. Amplitudes in centimetres, phases in degrees.

Cartwright *et al.* (1991), on calculations by Haines *et al.* (1990) using the GEM-T2 gravity model. And, also as in our previous work, residual orbit errors in $\Delta\xi$ were modeled by slowly modulated sinusoids of frequency one cycle/revolution. This frequency is known to dominate the error in collinear differences (*see*, for example, Cartwright and Ray (1990), Fig. 1); all other major components of the orbit error that are induced by errors in the gravity model are removed when forming $\Delta\xi$ through collinear differencing (*e. g.*, Schrama, 1989). An important point is that, even though we are interested here only in the tides of the Mediterranean Sea, global altimeter data were used to solve for orbit errors; had data from only the Mediterranean been used, the tidal signal and the orbital errors in $\Delta\xi$ would have remained hopelessly coupled.

Altimetric tidal analysis

The Geosat altimeter, passing over any particular point on its groundtrack every 17.05 days, causes each tidal constituent to be severely aliased into long-period oscillations (Parke *et al.*, 1987). Table 1 in both Cartwright and Ray (1990) and Woodworth and Thomas (1990) lists the alias periods for the major constituents, and they range from 52 days (N_2) to 317 days (M_2), excepting P_1 which is nearly frozen at a constant phase. Of all the gravitational tides, the ones of closest alias period to M_2 are K_1 at 175 days and S_2 at 169 days. Given two years of altimeter data, as in the present analysis, M_2 is easily separable from all other constituents according to the classical Rayleigh criterion and can be safely extracted alone. Within the M_2 tidal group, containing spectral lines differing in frequency by less than one cycle per month, there are no lines of importance except for the strong nodal line near the primary M_2 line, and it can be handled in the usual fashion (see below). The one tide not completely separable from M_2 in two years of data is the (primarily meteorological) annual Sa tide. It has a typical amplitude of about 5 cm in the central Mediterranean (Pattullo *et al.*, 1955; Woodworth, 1984; Rickards, 1985), a substantial fraction of M_2. High evaporation rates, thermal forcing, and runoff in the eastern and western basins may induce even stronger Sa amplitudes; indeed, Sa at Port Said has an amplitude of 11.5 cm according to the IHO constants. Nevertheless, the tides M_2 and Sa are separable if allowance is made for the spatial autocorrelation of each tide, as in our analysis. Even though 17.05 days are required for Geosat to return to a particular point, it passes within 1.47° to the east of that point in 3.005 days, in which time the phase of M_2 changes by nearly 70° (Cartwright and Ray, 1990, Tab. 1) whereas Sa remains essentially fixed. The spatial continuity of the Proudman functions thus enforces a separation of M_2 and Sa except at those locations where the functions are too rapidly varying, as in perhaps the Adriatic and possibly the Sicilian Strait.

The height of the M_2 tidal constituent at a given location and time may be expressed as

$$\xi(\varphi, \lambda, t) = f(t)\, H(\varphi, \lambda) \cos[\sigma t + V_0 + u(t) - G(\varphi, \lambda)] \quad (5)$$

where φ and λ are latitude and longitude, respectively, H is the M_2 amplitude and G the Greenwich phase lag when t is Universal Time, σ is the tidal speed (28.984° h^{-1}) and V_0 is the equilibrium argument corresponding to the origin of t. The nodal corrections f and u account for secondary spectral lines within the constituent; they may be taken as constant for periods up to six months or so, but since the Geosat ERM lasted three years, we incorporated continuous time variation in f and u according to Table 26 of Doodson (1928). For the entire Geosat mission (1985-1989), f for M_2 varied between 0.963 and 0.977, and u between - 1.6° and + 1.4°.

Equation (5) may be expressed in terms of an expansion in Proudman functions as

$$\zeta(\varphi, \lambda, t) = f(t) \cos[\sigma t + V_0 + u(t)] \sum_{n=1}^{N} a_n \phi_n(\varphi, \lambda) + f(t) \sin[\sigma t + V_0 + u(t)] \sum_{n=1}^{N} b_n \phi_n(\varphi, \lambda). \quad (6)$$

Because of equation (4), the altimeter observations, however, are of $\Delta\xi$, which may be expressed in similar form:

$$\Delta\zeta(\varphi, \lambda, t) = f(t) \cos[\sigma t + V_0 + u(t)] \sum_{n=1}^{N} a'_n \phi_n(\varphi, \lambda) + f(t) \sin[\sigma t + V_0 + u(t)] \sum_{n=1}^{N} b'_n \phi_n(\varphi, \lambda). \quad (7)$$

The functions $f(t)$ and $u(t)$ are sufficiently slowly varying that we have taken $f(t) = f(t + n\tau)$ and $u(t) = u(t + n\tau)$, satisfactory for our present choice of n = 2. Equation (7) can be solved by least squares for the coefficients a'_n and b'_n. Transformation to a_n and b_n, and thus by (3) to H and G, can then be had *via*

$$a_n = 1/2\, a'_n + 1/2\, b'_n \cot(\sigma n \tau 2)$$
$$b_n = 1/2\, b'_n + 1/2\, a'_n \cot(\sigma n \tau 2) \quad (8)$$

In the least-squares solution of (7), 1,588 Geosat passes of collinear differences were used, comprising some 160,000

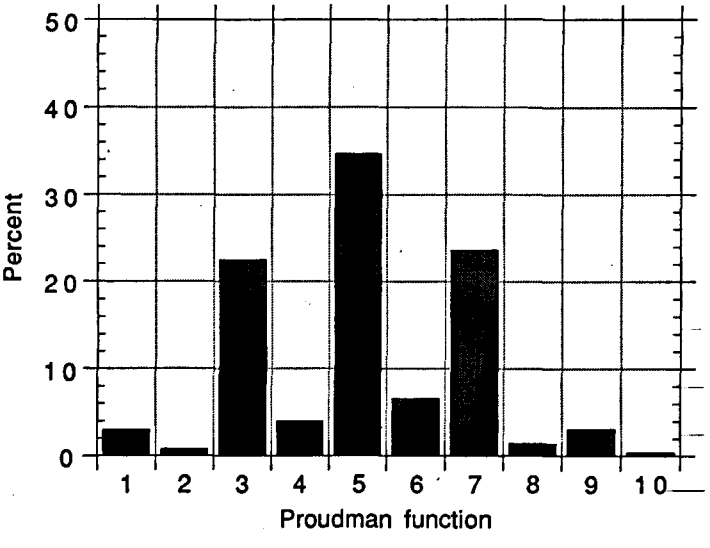

Figure 8

Percentage of potential energy contributed by each Proudman function in the fit to altimeter data only.

Table 3

Fit statistics for altimetry only.

N	Variance reduction (cm^2)
5	7.34
6	7.68
8	9.04
10	9.43
12	9.48
14	9.62

observations of $\Delta\xi$. The degree of fit N was chosen by noting its effect on the reduction in variance of $\Delta\xi$, shown in Table 3. This reduction begins to level off near $N = 10$, so we chose this value, which is also consistent with the choice for the tide-gauge fits. The rms residual for these collinear data was 13.3 cm; the overall altimeter noise was thus much stronger than the tidal signal in this area.

Maps of the M_2 amplitude and phase as derived from the altimetry are shown in Figure 7. The potential energy contributions from each mode in the solution is shown in Figure 8. The tide maps are seen to be quite similar in overall structure to the maps in Figure 3, although with some areas of discrepancy. Further discussion of these figures is again deferred to the final section.

COMBINED ALTIMETER-GAUGE SOLUTION

In Cartwright and Ray (1990; 1991), the global tide was determined by independent tidal analyses in small (1° x 1.475°) adjoining bins. The alternative use of spatial basis functions, such as the Proudman functions, allows disparate observations to be combined in a more straightforward manner (inverse methods based on *a priori* covariances also allow straightforward combination of disparate data, *see* Jourdin *et al.*, 1991). Such a combination of altimeter data and tide-gauge constants is described in the present section.

Combining normal equations from the separate altimetric and tide-gauge analyses is simple, but with two minor complications. The transformation represented by equations (8) must be duly accounted for, so that both sets of normal equations yield either (a_n, b_n) or (a'_n, b'_n). Secondly, realistic weights are required, not only to ensure that each data type properly influences the solution according to data quality, but also to yield an accurate error covariance matrix for deriving realistic standard errors for the tidal maps.

For altimeter data, the most elegant approach to weighting requires construction of a full (in contrast to a diagonal) least-squares weight matrix, which can properly account for autocorrelations in the observations (*e. g.*, Mazzega and Houry, 1989). With 160,000 observations, however, the computational burden of this approach necessitates some

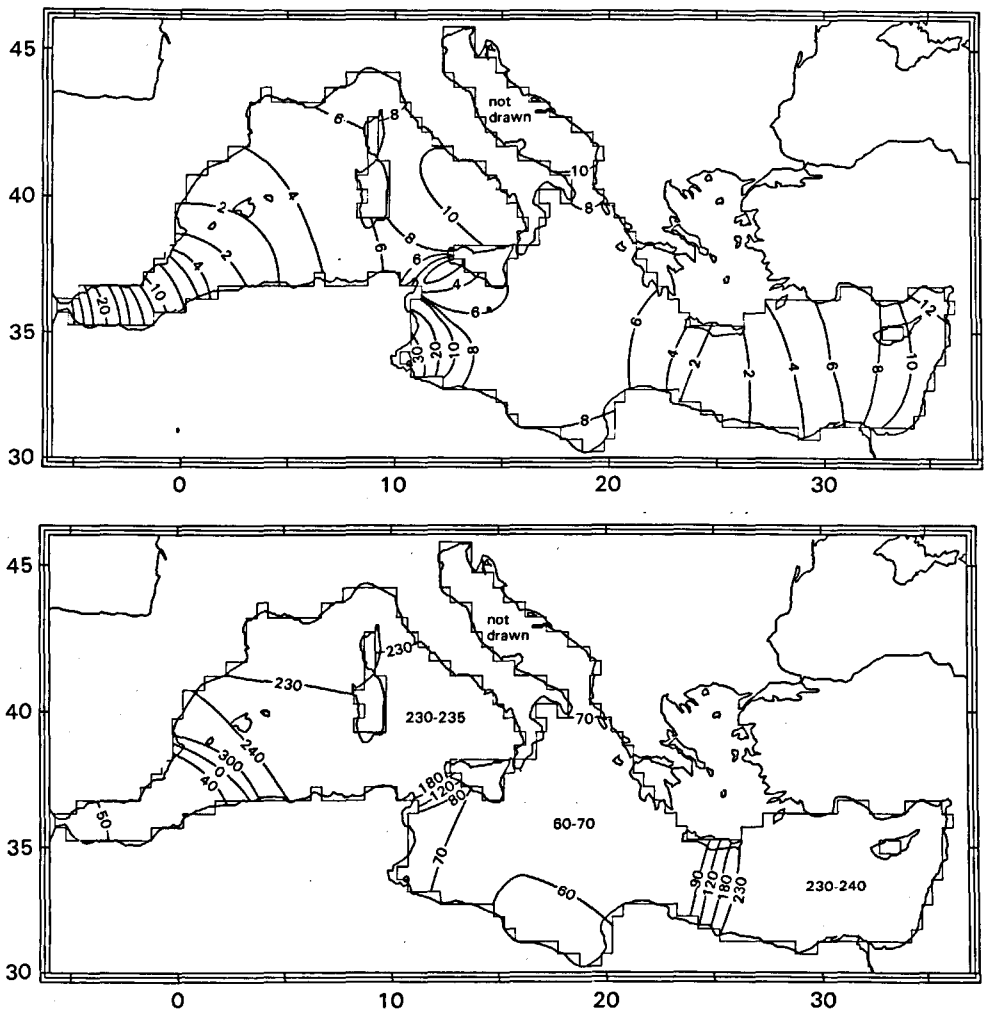

Figure 9

M_2 amplitudes (top) and Greenwich phase lags (bottom) from a joint solution combining altimeter data and tide-gauge harmonic constants. Amplitudes in centimetres, phases in degrees.

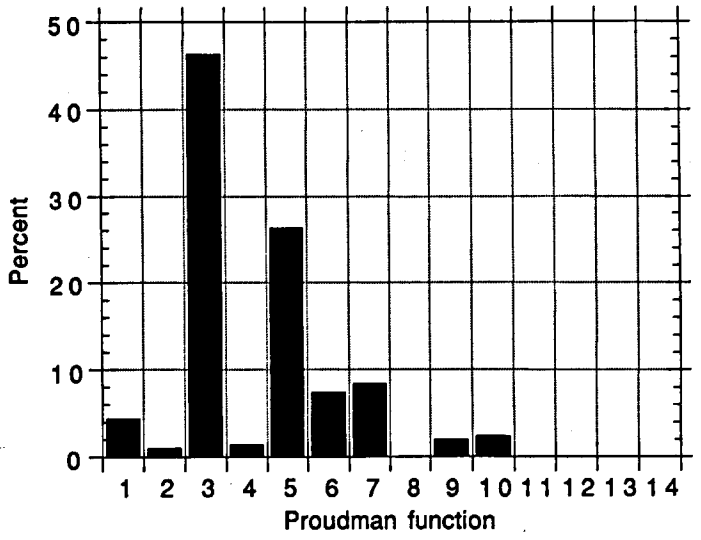

Figure 10

Percentage of potential energy contributed by each Proudman function in the combined (altimeter + tide-gauge) tidal solution. Compare Figures 4 and 8.

Standard errors (1-σ) in either the tidal in-phase or quadrature components (and the tidal amplitudes as well) were computed from the least-squares solution variance-covariance matrix (*e. g.*, Snedecor and Cochran 1989, § 17.8). They are shown in Figure 11. As might be expected, the high tide in the Gulf of Gabes is associated with the largest standard error. Figure 12 shows similar 1-σ standard errors for the altimeter-only solution. It too has large errors in the Gulf of Gabes, but also at the head of the Adriatic and in the Alboran Sea. The increased errors in these latter two areas clearly reflect the density of altimeter observations (Fig. 6).

DISCUSSION

In overall structure, the three sets of tidal maps, Figures 3, 7 and 9, look encouragingly similar, with the expected nodal structures near Alicante, Tunis, and Crete, and amplitude buildups on the eastern and western boundaries and in the Gulf of Gabes. In all three solutions, the predominant Proudman modes are function numbers 3,

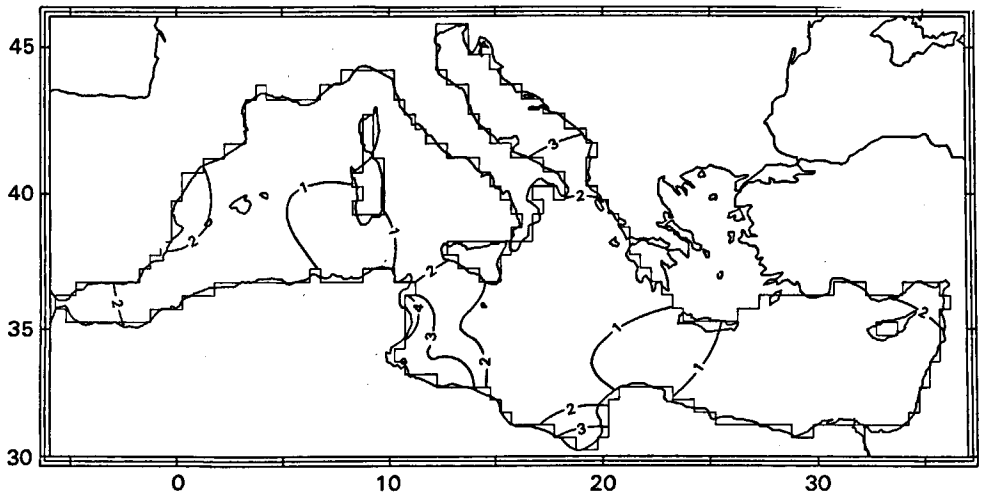

Figure 11

Standard errors (1-σ) in either the inphase or quadrature components of the M_2 tide, for the combined (altimeter + tide-gauge) solution. Contours in centimetres.

compromises. On the basis of Durbin-Watson statistical tests on (global) altimeter residuals, Ray and Koblinsky (1991) argued that the effective number of degrees of freedom in the altimeter data for estimation problems of this kind was of order 1 per 1 000 km of observations. For the Mediterranean Sea, this would imply that each of the 1 588 passes across the sea is associated with but 1 degree of freedom. Such heuristic reasoning leads us to set the weight of an altimeter observation as

$$\omega_A = (1\,588/160\,000) \times (1/13\text{ cm})^2 \approx 6 \times 10^{-5},$$

the 13 cm being the rms altimeter residual (for collinear data) cited in the previous section. For the tide-gauge data, we have taken the data variances as (3 cm)^2 according to Table 2, yielding a weight $\omega_T = 1/3^2 \approx 0.1$. Because by chance 160,000 ω_A is of order 86 ω_T, these weights cause both altimeter and tide-gauge data to contribute about equally to the combined normal equations. The combined tidal solution is shown in Figure 9. For additional flexibility, we had increased the degree of fit N to 14, but Figure 10 shows that the four additional modes contribute little to the solution.

5, 6, and 7. Function 3, with a computed period of 11.2 hours, is the non-rotational analogue of Schwab and Rao's normal mode of 11.4 h, and would be expected to respond in near resonance to the nearby semidiurnal tidal forcing. On geometrical grounds, Proudman function 6 is likewise expected to contribute, since its shape in the Gulf of Gabes most closely matches the sharp tidal resonance there.

Most of the differences in the tidal solutions can be attributed to poor coverage in the altimeter data. This is certainly so in the Alboran Sea where Figure 6 indicates the altimeter data are sparse; the altimeter-derived tide is therefore unconstrained near Gibraltar. Now according to Table 1, Proudman function 7 is most energetic in the Balearic and Alboran basins, so the lack of data there causes function 7 to be generally less well determined. In fact, in the altimeter fit, standard errors in the (a_n, b_n) coefficients for function 7 were 35 % larger than those for any other mode. The lack of data apparently allows function 7 to contribute unduly to the altimeter solution, which is evident in Figure 8. Elsewhere, differences in the tidal

Figure 12

Similar to Figure 11, but for the altimeter-only solution. Contours in centimetres. Increased errors in the Alboran and Adriatic Seas reflect sparsity of data as shown in Figure 6.

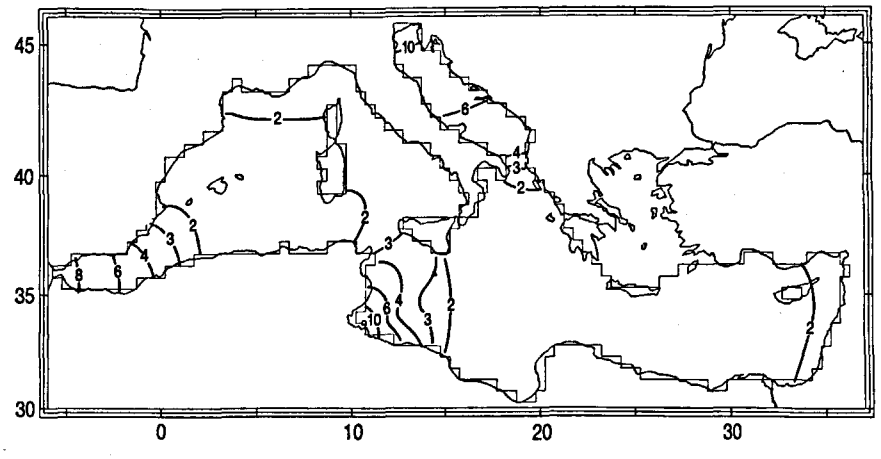

solutions are to be expected at the coast near Gabes because the altimeter groundtracks approach no closer than about 100 km from the head of the gulf. Other differences in tidal phases in areas of low amplitude are, of course, of no consequence in empirical maps.

The one puzzling area of discrepancy is in the far eastern basin where the altimeter solution is 4-5 cm lower amplitude and about 15° leading in phase relative to the tide-gauge solution. This may be due to a combination of causes. No Proudman function in Figure 1 displays a notable intensification in amplitude near the eastern boundary, except function 3, and it is only moderate. The altimeter coverage, more dense to the west of Cyprus than to the east, may be more heavily influenced in its fit to mode 3 by the lower amplitude tides to the west. But the tide-gauge fit is also somewhat inferior at Beirut, especially in phase, where Defant (1961) gives (H, G) = (13.4 cm, 233°). The most accurate solution may well be a combination of the altimeter-derived phases and the gauge-derived amplitudes, which in fact is fairly well what the combined solution of Figure 9 represents.

As noted in our discussion of the Proudman functions, one area of expected difficulty in all three tide solutions is the western Alboran Sea, where the artificially closed Strait of Gibraltar prohibits possible influences from the Atlantic Ocean. Indeed, the gauge-only solution is found to underestimate the amplitude at Gibraltar by nearly 7 cm, whereas the fit to the station east of Gibraltar (Malaga) is within 2 cm. With relatively deep bathymetry all the way to the closed strait, none of the Proudman functions of Figure 1 displays the strong gradients west of 4°W that are apparently required to model the increased amplitudes there. In fact, local observations indicate a strong east-west gradient both at Gibraltar and throughout the Strait (Candela *et al.*, 1990), with amplitudes increasing to nearly 1 m in the open Atlantic. In order to match the tidal measurements near Gibraltar and throughout the Alboran, one could alter the bathymetry in the neighborhood of Gibraltar by creating an artificial shallow shelf which would produce Proudman functions with the required structure.

Finally, it is of interest to compare the present altimeter results to those of Cartwright *et al.* (1991) who, as part of a global tidal solution for both diurnal and semidiurnal tides, give M_2 results in the Mediterranean (their Fig. 9). These previous results were somewhat noisy and allowed only a 10-cm contour line to be drawn. However, the entire western region from Sicily to southwest of the Balearic Islands was given amplitudes in excess of 10 cm, which is not in accord with either our tide-gauge or our altimeter results. The tidal phases in the central Mediterranean also disagree by 50°-100°. The results in Cartwright *et al.* were obtained by binning altimeter observations into small (1° x 1.48°) areas and performing independent tidal analyses in each. We may conclude that, in an area such as the Mediterranean, where the tide is small (indeed, smaller in rms than the altimeter noise level) and the data sometimes sparse (Fig. 6), the use of spatial basis functions is to be preferred. And the ability of Proudman functions to efficiently model kinematic features of the tide, unlike more analytic and/or isotropic functions, is a strong argument on their behalf.

Acknowledgements

We thank Brian Beckley and Anita Brenner for their help in maintaining the altimeter database in the Space Geodesy Branch at Goddard Space Flight Center. We also thank Bill Cunningham for programming and graphics support. Philip Woodworth confirmed for us the tidal constants at Palma, Mallorca. This work was partially funded by the NASA Topex/Poseidon Project.

REFERENCES

Candela J. (1989). Tidal and subinertial flows through the Strait of Gibraltar, *Ph. D. Dissertation, University of California, San Diego, USA*, 82 pp.

Candela J., C. Winant and A. Ruiz (1990). Tides in the Strait of Gibraltar. *J. geophys. Res.*, **95**, 7313-7335.

Cartwright D.E. and R.D. Ray (1990). Oceanic tides from Geosat altimetry. *J. geophys. Res.*, **95**, 3069-3090.

Cartwright D.E. and R.D. Ray (1991). Energetics of global ocean tides from Geosat altimetry. *J. geophys. Res.*, **96**, 16897-16912.

Cartwright D.E., R.D. Ray and B.V. Sanchez (1991). Oceanic tide maps and spherical harmonic coefficients from Geosat altimetry. NASA Tech. Memo. 104544, Goddard Space Flight Center, Greenbelt, 74 pp.

Cheney R.E., B.C. Douglas, R.W. Agreen, L. Miller, D.L. Porter and N. Doyle (1987). Geosat altimeter geophysical data record user handbook. NOAA Tech. Memo. NOSNGS-46, US Dept. of Commerce, Rockville, 28 pp.

Cheney R.E., B.C. Douglas, R.W. Agreen, L. Miller and N. Doyle (1988). The NOAA Geosat geophysical data records: summary of the first year of the Exact Repeat Mission. NOAA Tech. Memo. NOS NGS-48, US Dept. of Commerce, Rockville, 20 pp.

Defant A. (1961). *Physical Oceanography, vol. 2*. Pergamon Press, 598 pp.

Doodson A.T. (1928). The analysis of tidal observations. *Phil. Trans. R. Soc.*, **227**, 223.

Dressler R. (1980). Hydrodynamisch-numerische Untersuchungen der M_2 Gezeit und einiger Tsunamis im europäischen Mittelmeer. Mitteilungen d. Inst. für Meereskunde, Universität Hamburg, Nr. 23, 27 pp.

Farrell W.E. (1972). Deformation of the Earth by surface loads. *Revs Geophys. Space Phys.*, **10**, 761-797.

Garrett C. and F. Majaess (1984). Nonisostatic response of sea level to atmospheric pressure in the eastern Mediterranean. *J. phys. Oceanogr.*, **14**, 656-665.

Haines B.J., G.H. Born, G.W. Rosborough, J.G. Marsh and R.G. Williamson (1990). Precise orbit computation for the Geosat Exact Repeat Mission. *J. geophys. Res.*, **95**, 2871-2885.

Hansen W. (1962). Hydrodynamic methods applied to oceanographic problems. Mitteilungen d. Inst. für Meereskunde, Universität Hamburg, Nr. 1, 25-34.

Jourdin F., O. Francis, P. Vincent and P. Mazzega (1991). Some results of heterogeneous data inversions for oceanic tides. *J. geophys. Res.*, **96**, 20267-20288.

Maloney W.E. and R.E. Burns (1958). A reappraisal of the tides of the Mediterranean. US Navy Hydrographic Office, Tech. Rep. TR-61, Washington, D. C., 32 pp.

Marsh J.G. and T. Martin (1982). The Seasat altimeter mean sea surface. *J. geophys. Res.*, **87**, 3269-3280.

Mazzega P. and S. Houry (1989). An experiment to invert Seasat altimetry for the Mediterranean and Black Sea mean surfaces. *Geophys. J.*, **96**, 259-272.

Mosetti F. and N. Purga (1989). The semi-diurnal tides in the Sicily Strait. *Nuovo Cim.*, **12 C**, 349-355.

Mosetti F. and N. Purga (1990). Tides and sea level evolution at Alexandria (Egypt). *Nuovo Cim.*, **13 C**, 647-651.

Parke M.P., R.H. Stewart, D.L. Farless and D.E. Cartwright (1987). On the choice of orbits for an altimetric satellite to study ocean circulation and tides. *J. geophys. Res.*, **92**, 11693-11707.

Pattullo J., W. Munk, R. Revelle and E. Strong (1955). The seasonal oscillation in sea level. *J. mar. Res.*, **14**, 88-156.

Purga N., F. Mosetti and E. Accerboni (1979). Tidal harmonic constants for some Mediterranean harbours. *Boll. Geofis. teor. appl.*, **21**, 72-81.

Rao D.B. and D.J. Schwab (1976). Two dimensional normal modes in arbitrary enclosed basins on a rotating earth: application to Lakes Ontario and Superior. *Phil. Trans. R. Soc.*, **281**, 63-96.

Ray R.D. and B.V. Sanchez (1989). Radial deformation of the Earth by oceanic tidal loading. NASA Tech. Memo. 100743, Goddard Space Flight Center, 49 pp.

Ray R.D. and C.J. Koblinsky (1991). On the sea-state bias of the Geosat altimeter. *J. atmos. ocean. Technol.*, **8**, 397-408.

Ray R.D., C.J. Koblinsky and B.D. Beckley (1991). On the effectiveness of Geosat altimeter corrections. *Int. J. Remote Sens.*, **12**, 1979-1984.

Rickards L.J. (1985). Report on sea level data collected during the Medalpex Experiment, September 1981-September 1982. Institute of Oceanographic Sciences Report No. 209, Bidston, UK.

Sanchez B.V. and D.E. Cartwright (1988). Tidal estimation in the Pacific with application to Seasat altimetry. *Mar. Geod.*, **12**, 81-115.

Sanchez B.V., D.B. Rao and P.G. Wolfson (1985). Objective analysis for tides in a closed basin. *Mar. Geod.*, **9**, 71-91.

Schrama E.J.O. (1989). The role of orbit errors in processing of satellite altimeter data. Netherlands Geodetic Commission, Publications on Geodesy, New Ser., No. 33, Delft, 167 pp.

Schwab D.J. and D.B. Rao (1983). Barotropic oscillations of the Mediterranean and Adriatic Seas. *Tellus*, **35A**, 417-427.

Schwiderski E.W. (1983). Atlas of ocean tidal charts and maps. I: The semidiurnal principal lunar tide M_2. *Mar. Geod.*, **6**, 219-265.

Snedecor G.W. and W.G. Cochran (1989). *Statistical Methods, 8th ed.* Iowa State University Press, 503 pp.

Woodworth P.L. (1984). The worldwide distribution of the seasonal cycle of mean sea level. Institute of Oceanographic Sciences Report No. 190, Bidston, UK, 94 pp.

Woodworth P.L. and J.P. Thomas (1990). Determination of the major semidiurnal tides of the northwest European continental shelf from Geosat altimetry. *J. geophys. Res.*, **95**, 3061-3068.

Zahel W. (1970). Die Reproduktion gezeitenbedingter Bewegungsvorgänge im Weltozean mittels des hydrodynamische-numerischen Verfahrens. Mitteilungen d. Inst. für Meereskunde, Universität Hamburg, Nr. 17.